Spring 5-1-2022

When Problems Become Solutions: Harnessing the Osteogenic Capacity of Disease-Causing Stem Cells to Repair Bone Fractures

Mehreen Pasha
mehreenpasha19@gmail.com

When Problems Become Solutions: Harnessing the Osteogenic Capacity of Disease-Causing Stem Cells to Repair Bone Fractures

Mehreen Pasha

B.S. in Molecular and Cell Biology, Minor in Spanish

University Scholar Committee: Dr. David Goldhamer (Head), Dr. Geoffrey Tanner, Dr. Adam Zweifach

May 2022

Table of Contents

Abstract

While we often perceive disease as negative, there is potential to engineer seemingly negative biological phenomena into therapeutics to treat a variety of human illnesses. Fibrodysplasia ossificans progressiva (FOP) is a genetic disorder involving uncontrolled, widespread, extraskeletal bone growth, or heterotopic ossification (HO). In FOP patients, stem cells called fibro/adipogenic progenitors (FAPs) follow an abnormal, osteogenic pathway. In the present study, we investigate whether we can adapt these *Acvr1* mutant FAPs, which are exceptional at producing bone, to repair bone fractures in otherwise normal patients. The primary aims of this study are (1) to devise and optimize a novel method to simulate bone fractures less invasively in mice, and (2) to test whether mutant FAPs can form bone at fracture sites in a controlled and localized manner. Through micro-CT, we visualize and quantify ectopic bone volumes and observe that mutant FAPs form HO in both immunocompromised, SHO-*Prkdc*^{scid}*Hr*^{hr} (SCID) hosts and *Acvr1*$^{tnR206H/+}$;*R26*$^{NG/+}$;Tie2-Cre mice. However, HO does not appear to be highly localized to bone fragments without the use of activin A monoclonal antibody. Promisingly, donor bone fragments remain stable until at least 28 days post-transplantation. Notably, one replicate exhibited a remarkable increase in bone volume and change in morphology by day 14 followed by a decrease in bone volume by day 21 post-transplantation. Future work should involve the use of activin A monoclonal antibody, a greater number of bone fragments to maximize available bone morphogenetic proteins (BMPs), histological analyses to visualize cell populations contributing to bone fragment changes (both stem cells and immune

populations), and additional trials. Ultimately, this study is an innovative way to adapt an aberrant process to treat another ailment.

Acknowledgments

I am immensely grateful for the mentorship and support I received under the guidance of Dr. David Goldhamer, from composing my IDEA Grant to applying to medical school to graduating as a University Scholar. I am a better researcher and writer because of Dr. Goldhamer's invaluable feedback and expertise.

I want to thank my graduate student mentor, Lorraine Apuzzo, for teaching me essential techniques throughout the evolution of my project and entrusting me with both exciting and rigorous lab work. I also want to thank Erik Choi for the camaraderie and collaboration in lab. Thank you for making every day brighter and being the best friend and lab mate.

I deeply appreciate the assistance of everyone in lab, past and present: Masa, Cathy, Youfen, Tony, Cory, Sean, Amanda, Russ, Brenden, Sam, Heather, Amy, and Rayna. Spending almost every day with all of you, whether at the benchtop, carrels, or mouse room, was a defining part of my undergraduate career. I will never forget the iconic atmosphere you all cultivated both inside and outside lab.

Other faculty members whom I would like to give my thanks are Dr. Geoffrey Tanner and Dr. Adam Zweifach for serving on my University Scholar Committee as well as Dr. Thomas Abbott for providing advice about how to find a research laboratory as a first semester

freshman, which led me to the Goldhamer Lab where I spent the past three and a half years. I would also like to acknowledge Dr. Monica van Beusekom (University Scholar Program), Melissa Berkey (UConn IDEA Grant Program), and Dr. Anne Kim (STEM Scholar Community) for their assistance navigating these programs. My project would also not be possible without the funding provided through the UConn IDEA Grant Program.

I am deeply grateful for the lifelong support of my family and friends thus far and as I embark on my next academic journey. I want to thank my parents, Drs. Mohammad Akbar Pasha and Saima Pasha; sisters, Aisha, Zara, and Rafia; cousins; and aunts and uncles, especially Mohammad Anwar Pasha. Thank you to my fellow University Scholar Mehak Sharma for being the best roommate and friend. Lastly, thank you to my best friend, Tamashi Hettiarachchi, for being there for me unwaveringly from freshman orientation to graduation and beyond. Thank you for ensuring my writing was accessible to a general audience as well as supporting and celebrating my academic and personal adventures. You all have been an integral part of my growth as a person.

Introduction

The role of *Acvr1* mutant fibro/adipogenic progenitors (FAPs) in fibrodysplasia ossificans progressiva (FOP)

Fibrodysplasia ossificans progressiva (FOP) is a genetic disorder involving uncontrolled, widespread, extraskeletal bone growth known as heterotopic ossification (HO) (Lees-Shepard *et*

al., 2018a). Patients with FOP experience limited mobility and, in more severe cases, difficulty opening their mouth if bone forms in the jaw (resulting in malnutrition) and trouble breathing if bone forms in the thoracic cavity, leading to high morbidity (Kaplan *et al.,* 2008).

FOP stems from a single amino acid change from arginine to histidine at position 206 (R206H) in the ACVR1 protein (Shore *et al.,* 2006). The gene *Acvr1* encodes bone morphogenetic protein (BMP) type I receptor (Shore *et al.,* 2006). Normally, BMP ligands (which are present near bone) bind to BMP type I receptors and trigger a signaling cascade that leads to osteogenesis, or bone formation (Lees-Shepard *et al.,* 2018a). The *Acvr1* mutation makes bone growth go awry because it causes the BMP type I receptor to become hypersensitive to BMPs (Culbert *et al.,* 2014; Shen *et al.,* 2009), resulting in robust and widespread bone growth (Lees-Shepard *et al.,* 2018b). Furthermore, the mutation in the *Acvr1* gene alters the activity of another protein known as activin A (Hatsell *et al.,* 2015), which is ubiquitously expressed. Normally, activin A binds to the ACVR1 receptor, triggers a signaling pathway known as SMAD2/3 which inhibits BMP signaling, and leads to less bone growth (Hino *et al.,* 2015). However, in FOP, when activin A binds to the ACVR1 mutant complexes, it activates osteogenesis instead of inhibiting it (Lees-Shepard *et al.,* 2018b; Hatsell *et al.,* 2015; Hino *et al.,* 2015). It is believed that the mutant receptor perceives activin A as a BMP ligand (Wolken *et al.,* 2018). Interestingly, activin A is an obligatory ligand for bone formation in FOP (Lees-Shepard *et al.,* 2018b; Hatsell *et al.,* 2015).

Fibro/adipogenic progenitor biology and their role in FOP pathogenesis

Our lab has recently identified a major contributing cell type to FOP called fibro/adipogenic progenitors (FAPs), multipotent, mesenchymal stem cells that reside in the muscle interstitium (Contreras *et al.,* 2021). They are characterized by the expression of platelet-derived growth factor receptor alpha (PDGFRα), stem cell antigen-1 (Sca-1) (Joe *et al.,* 2010), and cluster of differentiation 34 (CD34) (Giordani *et al.* 2019); however, they are CD31 and CD45 negative (Molina *et al.,* 2021). These criteria are used to isolate FAPs from other muscle-resident cell types.

FAPs communicate cellularly and molecularly with various cell types present in muscle. Importantly, they interact with satellite cells, or muscle stem cells (Mauro 1961; Molina *et al.,* 2021). Satellite cells assume a myogenic fate to regenerate injured skeletal muscle. If FAPs are depleted, satellite cell numbers decrease after nine months (Wosczyna *et al.,* 2019). FAPs help facilitate myogenesis through the release of extracellular matrix (ECM) and immune-related signaling factors (Scott *et al.,* 2019; Molina *et al.,* 2021). FAPs express chemokines and cytokines that affect neutrophils, monocytes, and other immune cell types (Oprescu *et al.,* 2020). In fact, there is a positive correlation between inflammatory cell numbers and FAPs proceeding injury (Molina *et al.,* 2021).

Previous research investigates the role of FAPs in normal skeletal muscle repair and regeneration. However, in many pathogenic contexts, they can differentiate into fibroblasts, adipocytes, as well as osteogenic and chondrogenic cells depending on the presence or absence of specific signaling factors in the environment (Joe *et al.,* 2010; Uezumi *et al.,* 2010; Contreras

et al., 2021; Molina *et al.,* 2021). For instance, transforming growth factor-β (TGF- β) triggers fibrogenesis while dexamethasone, 3-isobutyl-1-methylxanthine, and insulin induce adipogenesis (Uezumi *et al.,* 2011; Molina *et al.,* 2021). FAPs can undergo osteogenesis in the presence of BMPs 2, 7, or 9 (Wosczyna *et al.,* 2012; Lees-Shepard *et al.,* 2018b). In fact, Matrigel-BMP2 constructs containing FAPs form cartilage and bone *in vivo* (Wosczyna *et al.,* 2012). As previously discussed, activin A is necessary to stimulate *Acvr1*^{tnR206H} mutant FAPs to undergo endochondral ossification after skeletal muscle injury (Lees-Shepard *et al.,* 2018b). Normally, endogenous BMPs alone are not in sufficient quantity to stimulate osteogenesis in FAPs. If activin A is blocked using an activin A antibody, then it cannot bind to the abnormal type I BMP receptors and bone growth does not occur (Lees-Shepard *et al.,* 2018b).

Given that FAPs with the *Acvr1* mutation are exceptionally good at making bone and the location of this process can be controlled using an agent that blocks activin A activity, like an activin A antibody, a logical next step is to test whether we can take advantage of this ability and use mutant FAPs to generate bone in a healthy person with a bone fracture. This feature makes FAPs a particularly exciting future therapeutic. Their exceptional bone-producing property while in the presence of BMPs (which are abundant near fracture sites) has the potential to be "shut off" elsewhere by introducing an activin A antibody.

Cre-dependent knockin mouse model of FOP

Our lab has previously developed a mouse model of FOP in which *Acvr1*^{tnR206H} recombination is targeted to FAPs using Tie2-Cre (Lees-Shepard *et al.,* 2018b). Cre recombinase

is an enzyme that recombines DNA at specific sites. When manipulating genes, Cre cleaves at loxP sites that flank a sequence of DNA, leading to gene insertion, deletion, inversion, or translocation. Tissue or cell population specific Cre recombinases can be selected for spatial and temporal control over the expression of a mutation, such as Tie2-Cre which specifically targets FAPs as well as endothelial and hematopoietic stem cells (Kisanuki *et al.,* 2001; Puri and Bernstein, 2003; Takakura *et al.,* 1998). Conditional knockins (Figure 1) are beneficial when genetic mutations are lethal for the organism if expressed during embryogenesis or perinatally, as seen in FOP (Kaplan *et al.,* 2012). A tdTomato reporter stop cassette flanked by loxP sites in intron 4 of *Acvr1* not only prevents read-through transcription of the R206H mutation (located downstream in exon 5) without Cre recombinase, but also labels unrecombined cells red (Lees-Shepard *et al.,* 2018b); the CAG promoter/enhancer drives this stop cassette (Lees-Shepard *et al.,* 2018b). Our FOP mouse model enables us to determine recombination efficiency through fluorescent reporters (Lees-Shepard *et al.,* 2018b). $R26^{NG}$ indicates Cre expression and fluoresces green from green fluorescent protein (GFP) (Lees-Shepard *et al.,* 2018b). Without Cre, the stretch of DNA containing the tdTomato reporter stop cassette does not get excised, the *Acvr1* mutation characteristic to FOP does not get transcribed, and the unrecombined cells appear red (Lees-Shepard *et al.,* 2018b).

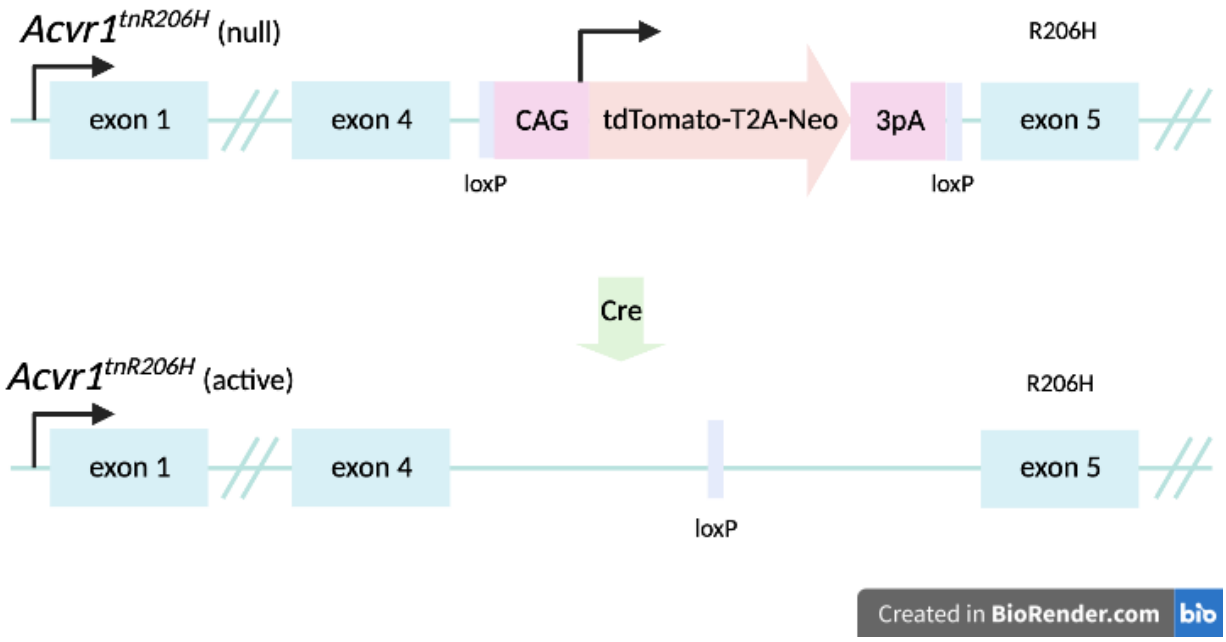

Figure 1: Schematic of our Cre-dependent knockin mouse model involving recombination of the *Acvr1*^{tnR206H} allele. Created with BioRender.com

Bone fractures: preexisting treatments and prevalence

Bone fractures and the surgical approaches that fix them have been an area of great investigation within regenerative medicine and orthopedics. Bone fractures are some of the most common orthopedic-related injuries, resulting from automobile accidents, falls, sports-related injuries, etc. While healing occurs during the 6-8 weeks post injury, complications—from excessive movement at the site of fracture to substance abuse—can prolong repair (Perez *et al.,* 2018).

Currently, the treatment of choice for nonunion fractures, which are severe fractures that do not heal without surgical intervention, is a bone graft—specifically autografts (coming

from the patient), allografts (coming from a donor), and synthetic grafts (derived from stem cells) (Perez *et al.,* 2018). However, each technique has numerous drawbacks in terms of their effectiveness, chance of further complications, and costs. Allografts can cause an infection or be rejected by the patient's immune system. They also require extensive sterilization which can diminish osteoconduction and osteoinduction (Cipriano *et al.,* 2019). Autografts, while solving the issue of immune rejection, have several drawbacks including morbidity at the donor site, muscle weakness, and surgical complications (Perez *et al.,* 2018). They are also more invasive due to the need for a second surgery to harvest the grafting tissue (Cipriano *et al.,* 2019). Synthetic grafts often cannot withstand long term wear and tear. In fact, as high as 60% of grafts fail (Perez *et al.,* 2018). Grafts are quite costly; approximately 1.6 million are administered in the U.S. every year, amounting to over $244 billion (Perez *et al.,* 2018).

Notably, traditional stem cell therapies involving bone marrow mesenchymal stem cells can be ineffective because they often lose their osteogenic ability when handled in the lab (unpublished data). Empirical evidence suggests that *Acvr1* mutant FAPs maintain their osteogenic capacity longer and perform better both in culture and *in vivo*. Investigating the potential therapeutic ability of these FAPs in treating bone fractures in otherwise normal patients is a fascinating clinical application.

Hypotheses and experimental aims

Our study seeks to determine whether mutant FAPs can be introduced in a localized fashion at the site of bone fracture in mice and repair bone in an efficient and controlled

manner. In addition, we want to know whether administering an antibody for activin A alongside mutant FAPs helps "shut off" mutant FAP activity farther away from the immediate fracture site. We hypothesize that, if *Acvr1* mutant FAPs are injected at the site of a bone fracture in mice, then mutant FAPs will assume an osteogenic fate and repair the fracture faster than mice injected with normal FAPs or traditionally used mesenchymal stem cells. Additionally, we hypothesize that, after mutant FAP introduction along with the activin A antibody, bone growth will only occur in the immediate vicinity of the fracture, where BMP ligands stimulate them to participate in bone repair. Our study also seeks to create and optimize a novel method to simulate bone fractures in mice without physically fracturing bones since such protocols are not well established in the mouse model. Instead of physically fracturing bones (which is invasive and requires particular analgesics), we hypothesize that transplanting bone fragments from a donor mouse into the gastrocnemius muscle of a host mouse can model a bone fracture at the cut ends of donor fragments.

Materials and Methods

Animals

SHO-*Prkdc*^{scid}*Hr*^{hr} and *Acvr1*$^{tnR206H/+}$;*R26*$^{NG/+}$;Tie2-Cre mice were housed and cared for in accordance with the University of Connecticut IACUC policies and procedures to ensure animal welfare. Mice were genotyped by checking for reporter fluorescence and conducting polymerase chain reaction (PCR).

Fluorescence-activated cell sorting (FACS) and cell injection

ACVR1(R206H)-expressing FAPs were obtained as previously described (Biswas and Goldhamer, 2016). Briefly, muscle dissociation buffer contains Dulbecco's Modified Eagle Medium (DMEM) (Life Technologies), 2 mg/mL Collagenase Type II (Worthington Biochemical) and 0.3 mg/mL Dispase (Invitrogen). Hindlimb muscle tissue was harvested and placed in enough dissociation buffer (Figure 2A) to facilitate mincing, which involved cutting the muscle tissue with scissors for 10 minutes and forming a paste-like consistency (Figure 2B). Samples resided in muscle dissociation buffer for approximately 1.5 hours with gentle trituration using a pipette and/or shaking every 15 minutes. Cold media containing 20% Fetal Bovine Serum (FBS) (R&D Systems) in DMEM was used to quench digestion. The solution was filtered using 100 µm and 70 µm strainers (Corning; Fisher Scientific) (Figure 2C) and underwent centrifugation. After further washing and resuspension as described (Biswas and Goldhamer, 2016), samples were incubated with the appropriate antibodies to isolate *Acvr1* mutant FAPs from other cell types present in hindlimb muscle. FAPs were separated based on the presence of PDGFRα and SCA-1 and the absence of myeloid and endothelial markers (CD45 and CD31, respectively) using the FACS Aria II (BD Biosciences) (Figure 2D). Mutant FAPs were separated from wild type by selecting cells not expressing tdTomato, demonstrating recombination. Approximately 450,000 FAPs were collected and cultured for transplantation. Ultimately, one dose of FAPs suspended in Dulbecco's Phosphate Buffered Saline (DPBS) (Life Technologies) was administered at 1×10^6 cells per 50 µL injection using an insulin syringe (Exel International) (Lees-Shepard *et al.,* 2018b).

Bone fragment transplantation

A bone fracture was simulated by embedding either one-4mm fragment or two-2mm fibular bone fragments into the gastrocnemius muscle of FOP mice (Figure 3). The former was conducted in SHO-*Prkdc*^{scid}*Hr*^{hr} mice before methods were optimized to increase the amount of exposed, cut bone by increasing the number of fragments to two. Bone fragments were collected from wild-type mice, serving as a scaffold and source of BMPs. A pilot hole was introduced using a 25-gauge needle (Fisher Scientific) intramuscularly to aid in fragment insertion. Bone fragments were inserted intramuscularly parallel to the grain of the gastrocnemius muscle, and bone volumes were quantified at 0, 7, 14, 21, and 28 days post-transplantation.

During pilot experiments in SHO-*Prkdc*^{scid}*Hr*^{hr} hosts, one bone fragment was inserted. The left hindlimb contained a bone fragment and mutant FAPs, while the right hindlimb contained only a bone fragment and served as a control to test whether wild-type resident FAPs would contribute at all to HO. Immunocompromised mice eliminate the issue of immune rejection when transplanting foreign cells (Lees-Shepard *et al.,* 2018b). To introduce more nucleation sites for potential HO, two fragments were transplanted when using *Acvr1*$^{tnR206H/+}$;*R26*$^{NG/+}$;Tie2-Cre hosts.

Cardiotoxin-mediated injury to trigger HO in *Acvr1*$^{tnR206H/+}$;*R26*$^{NG/+}$;Tie2-Cre mouse model

Cardiotoxin injury was conducted after administering isoflurane anesthesia to the mice. To trigger injury-induced HO in our FOP mouse model, 100 µL injections of 10 µM cardiotoxin

(Sigma) were conducted bilaterally into the mid belly of the gastrocnemius muscle the day prior to bone fragment transplantation (Figure 5).

Micro-CT

Under isoflurane anesthesia, mice were imaged at 0, 7, 14, 21, and 28 days post bone fragment transplantation (Figures 2 and 3)—ideal timepoints from our previous studies (Lees-Shepard *et al.,* 2018b)—using the IVIS SpectrumCT model 128201 (Perkin-Elmer) to see the mouse's bones in real time, confirm fragment presence, track bone fragment stability, and quantify FAP-mediated bone deposition. Assessing bone fragment stability was crucial to ensure processes like endogenous bone resorption or an innate immune response did not degrade the fragments. The setting employed on the IVIS SpectrumCT was medium resolution acquisition mode, which scans hindlimbs. 3D Slicer (http://www.slicer.org), a software that uses 3-D reconstruction to generate models for visualization and volumetric quantification, was utilized to determine bone volumes and pseudo color fragments and HO to generate images. This quantification of bone growth at each time point served as a metric to compare experimental (left) and control (right) limbs within the same mouse as well as across different replicates.

Results

Bone fragment transplantation and *Acvr1* mutant FAP injection into SHO-*Prkdc*^{scid}*Hr*^{hr} hosts form HO that is not highly localized to bone fragments

Hindlimb muscle tissue was harvested from FOP (*Acvr1*$^{tnR206H/+}$;*R26*$^{NG/+}$;Tie2-Cre) mice and dissociated to obtain a single cell suspension as previously described (Figure 2). Adherent cells were grown in culture prior to fluorescence-activated cell sorting (FACS) to isolate mutant FAPs (fluorescing green under a microscope for easy visualization) (Figure 2D).

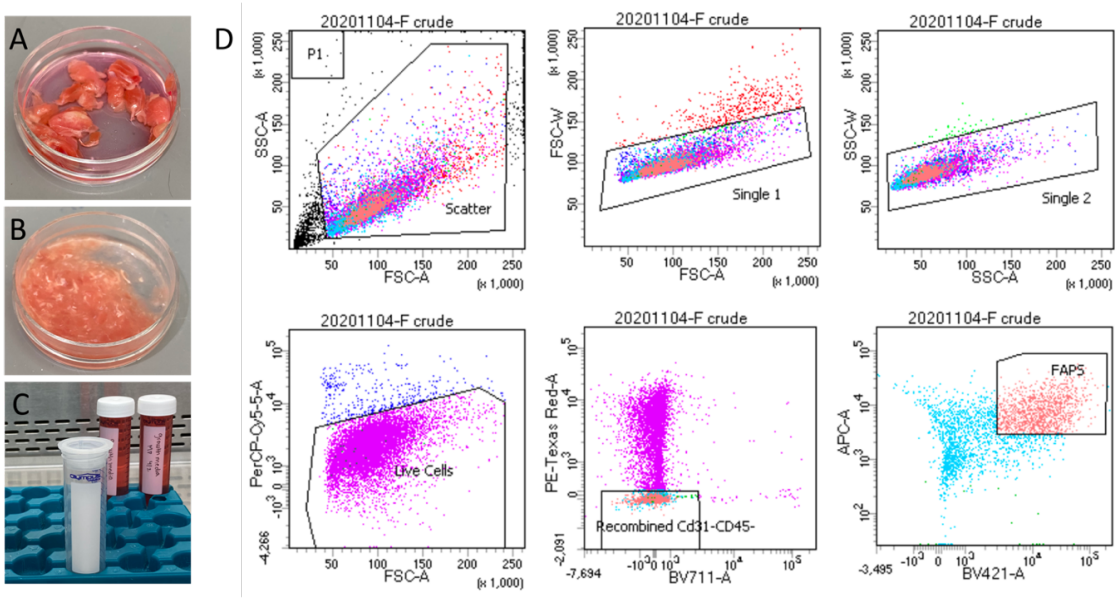

Figure 2: Muscle collection and fluorescence-activated cell sorting (FACS) gating strategy. (A) Harvested hindlimb muscle tissue in a 35 mm x 10 mm Petri dish containing enough muscle dissociation buffer to partially submerge the tissue. (B) Hindlimb muscle tissue proceeding approximately 10 minutes of mincing with scissors, resulting in a paste-like consistency. (C) Strainers (100 µm and 70 µm) used to filter solutions of dissociation media, cold media, and minced hindlimb muscle tissue. (D) FACS gating strategy for collection of TdTomato-/CD31-/CD45-/PDGFRα+/SCA-1+ FAPS. This mutant FAP subpopulation was grown in culture until enough cells were generated prior to intramuscular injection. FACS was conducted by graduate student mentor Lorraine Apuzzo.

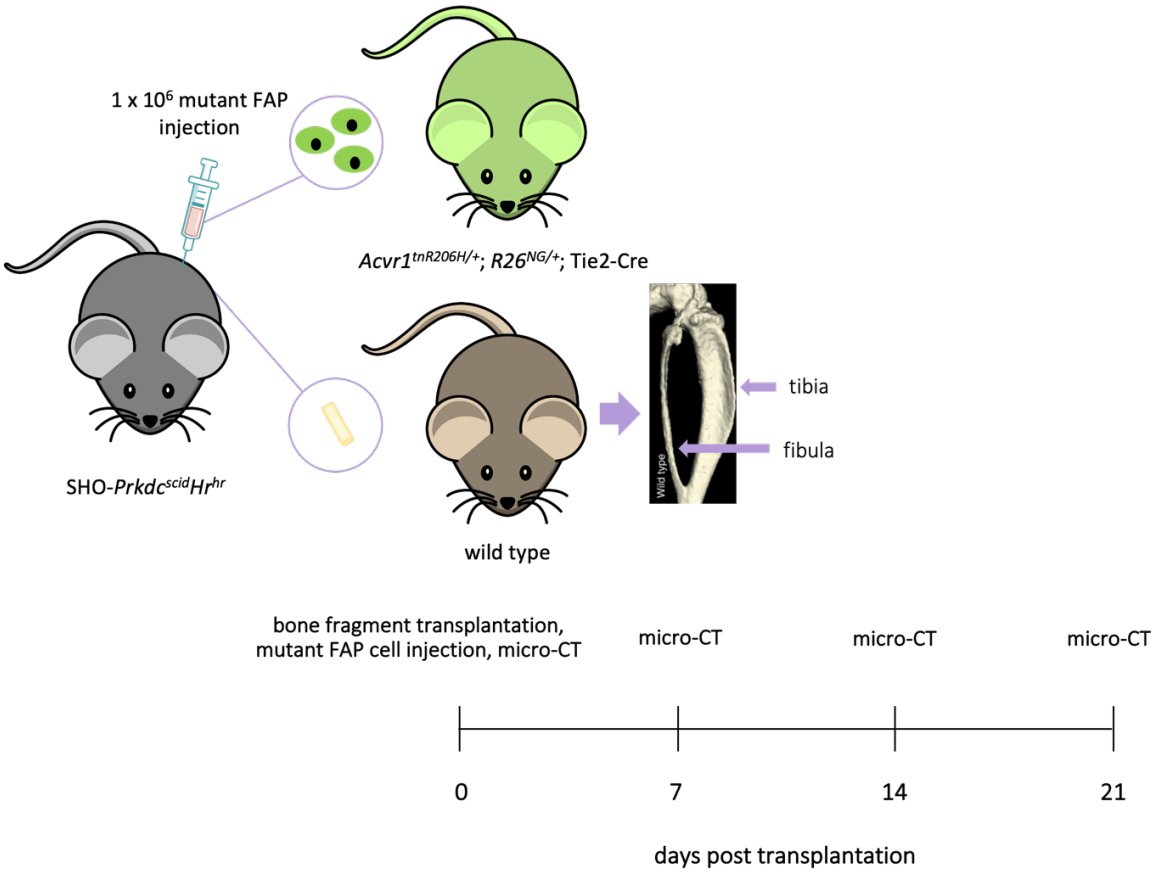

Figure 3: Schematic of bone fragment transplantation study workflow using SHO-*Prkdc*^{scid}*Hr*^{hr} hosts.

At day 14 post-transplantation of bone fragment and *Acvr1* mutant FAPs (Figure 3), ectopic bone growth was observed in the left hindlimb (LHL) in the absence of activin A monoclonal antibody (Figure 4A). However, it was not highly localized to the fragment (Figure 4A). LHL HO was 11.52 mm^3, 2.31 mm^3, and 7.79 mm^3 for trials 1, 2, and 3 respectively, demonstrating variability among replicates (Figure 4B). At day 14 post-transplantation, trial 1 had the highest HO volume but lowest fragment volume (0.83 mm^3); trial 2 had the lowest HO volume but highest fragment volume (2.31 mm^3); trial 3 had intermediate HO and fragment volumes (1.27 mm^3) (Figure 4B). In the right hindlimb (RHL) control, a bone fragment alone was

transplanted to track its stability without mutant FAPs present. RHL fragment volumes were relatively consistent at 1.59 mm^3, 1.24 mm^3, and 1.32 mm^3 for trials 1, 2, and 3, respectively (Figure 4B). Furthermore, endogenous wild-type FAP contribution was not observed due to the lack of HO in the right hindlimb at day 14 in all three trials (Figure 4B). Additional trials must be conducted to determine if the lack of HO localization to the bone fragments was a technical error or if the methodology needs to be amended. One potential source of high variability in HO in the LHL was technical error, namely cells settling in solution prior to transplantation.

D14 left hindlimb (bone fragment + mutant cells)

D14 right hindlimb (bone fragment only; control)

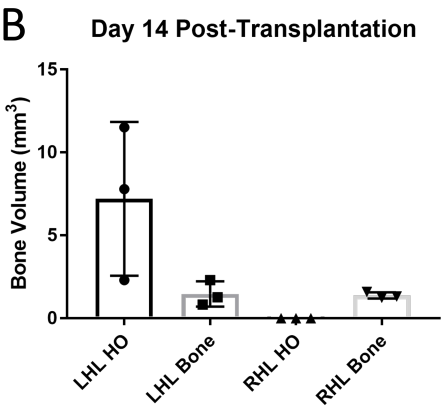

trial	LHL HO	LHL fragment	RHL HO	RHL fragment
1	11.52	0.83	0	1.59
2	2.31	2.31	0	1.24
3	7.79	1.27	0	1.32

Figure 4: Micro-CT quantification of bone growth (heterotopic ossification, HO) proceeding bone fragment and mutant FAP transplantation into an immunocompromised mouse. (A) At day 14 post-transplantation, mutant FAPs formed bone (blue) in the absence of activin A monoclonal antibody but did not co-localize with the transplanted bone fragments (red). (B) HO and bone fragment volumes (mm^3) were quantified for experimental (left hindlimb, LHL) and control (right hindlimb, RHL) samples. Statistics and additional trials pending. Micro-CT scans were processed and bone volumes were quantified by graduate student mentor Lorraine Apuzzo using 3D Slicer.

Bone fragment transplantation into *Acvr1*$^{tnR206H/+}$;*R26*$^{NG/+}$;Tie2-Cre hosts forms HO that is not highly localized to bone fragments

A different approach that we investigate here is to transplant bone fragments into host mice with endogenous mutant FAPs, namely mice with the FOP mutation, to circumvent localized cell transplantation (Figure 5). Bilateral cardiotoxin injections were conducted in the gastrocnemius muscles of *Acvr1*$^{tnR206H/+}$;*R26*$^{NG/+}$;Tie2-Cre hosts while bone fragments harvested from wild-type donors were transplanted into the left hindlimb only (Figure 5; Figure 6A, C, E, G). Since the host was not immunocompromised, immune rejection was a potential concern.

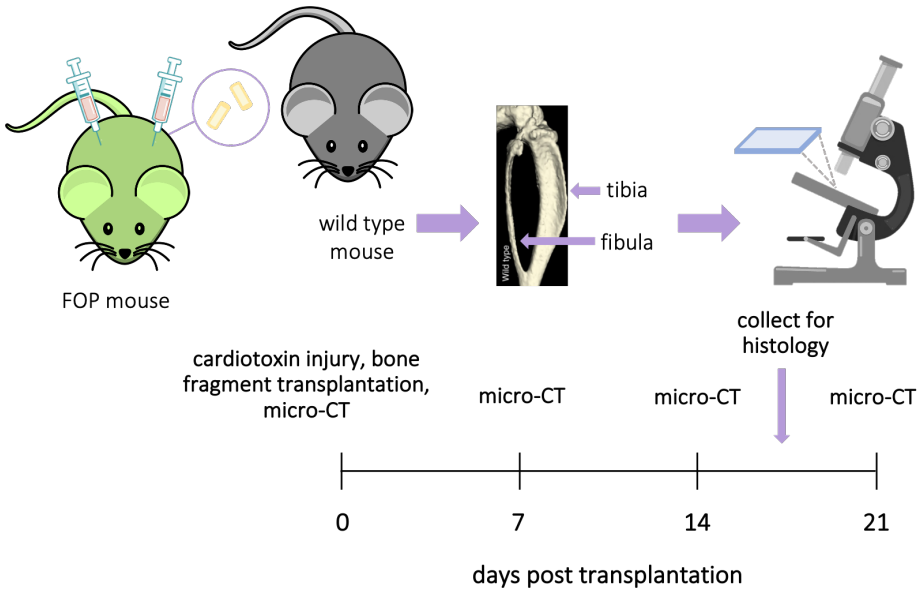

Figure 5: Schematic of bone fragment transplantation study workflow using *Acvr1*$^{tnR206H/+}$;*R26*$^{NG/+}$;Tie2-Cre hosts

In replicate 1, on day 14 post-transplantation, both fragments underwent morphological changes, as evidenced by the mushroom-like structure at the end of the pseudo-colored red fragment (Figure 6E). Between day 7 and 14, there was a dramatic increase in red bone

fragment size from 0.412594 mm^3 to 0.97875 mm^3 (Figure 9A-C). The blue fragment stayed relatively constant in bone volume between day 7 and 14, with volumes of 0.634922 mm^3 and 0.62859 mm^3, respectively (Figure 9A-C). Interestingly, both red and blue fragments decreased in volume between days 14 and 21 (Figure 9A-C). The blue fragment went from 0.62859 mm^3 to 0.424828 mm^3 while the red fragment went from 0.97875 mm^3 to 0.261141 mm^3 (Figure 9A-C). RHL HO also decreased from 26.9253 mm^3 to 16.6075 mm^3 in contrast to LHL HO, which increased from 27.3337 mm^3 to 31.201 mm^3 between day 14 and 21 (Figure 6B, D, F, H; Figure 9A-C). Scanning halted at day 21 due to the premature death of the host mouse.

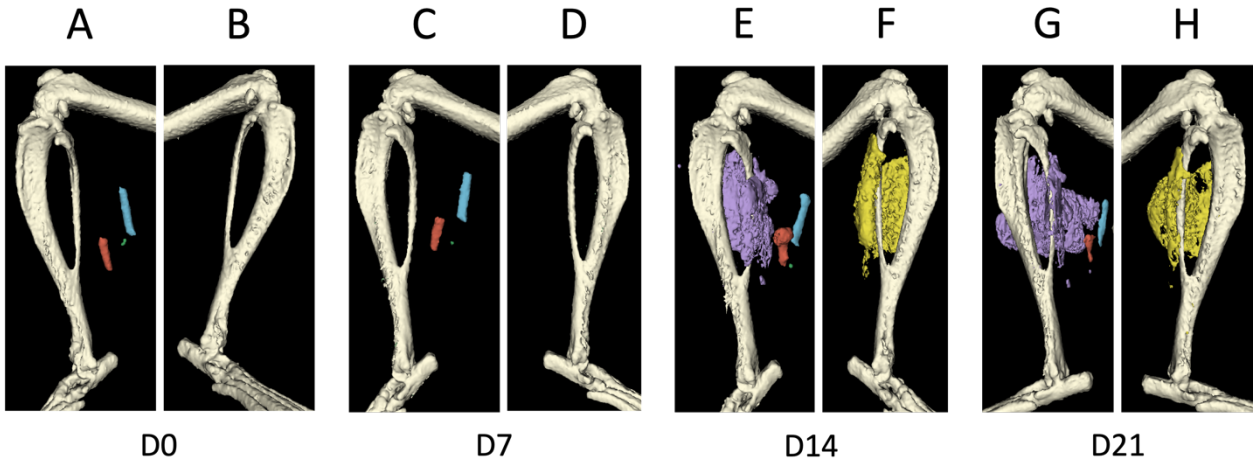

Figure 6: Replicate 1 micro-CT quantification of HO proceeding bone fragment transplantation into FOP host. Micro-CT conducted at days 0, 7, 14, and 21 post-transplantation revealed changes in bone volume and morphology of transplanted fragments as well as the presence of cardiotoxin-induced HO. Bone volume (mm^3) was quantified for experimental (LHL) and control (RHL) samples. Within each time point shown above, the left hindlimb is the left panel and the right hindlimb is the right panel. Note: images were cropped and resized to preserve consistent sizing of anatomical landmarks.

Replicate 2 also demonstrated fragment stability as well as changes in size and morphology (Figure 7A, C, E, G, I). LHL HO consistently increased between every time point while the blue fragment increased from day 0 to day 7 (0.391078 mm^3 to 0.462797 mm^3) but decreased steadily at all remaining time points; the red fragment also increased from day 0 to 7 (0.385594 mm^3 to 0.415547 mm^3) but steadily decreased from day 7 to day 28 (Figure 9A-C). RHL HO peaked at day 14 (2.54728 mm^3), decreased at day 21 (1.41539 mm^3), and increased again at day 28 (1.85161 mm^3) (Figure 7 B, D, F, H, J; Figure 9A-C).

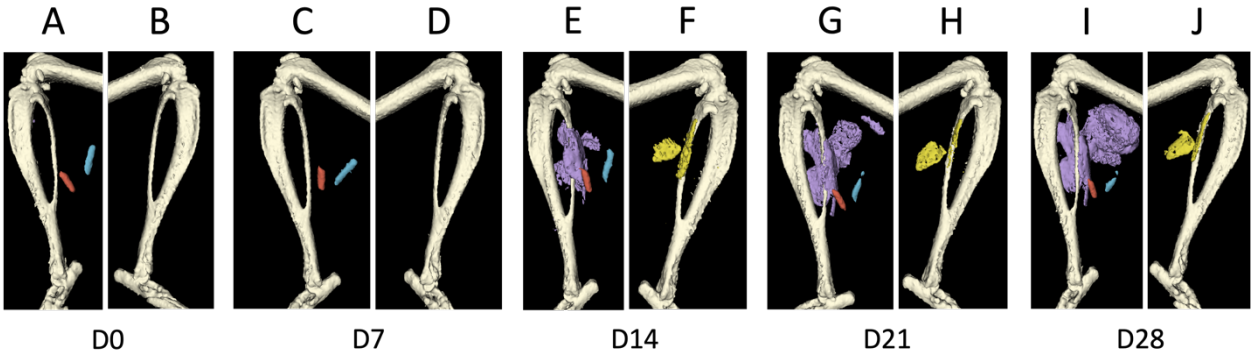

Figure 7: Replicate 2 micro-CT quantification of HO proceeding bone fragment transplantation into FOP host. Micro-CT conducted at days 0, 7, 14, 21, and 28 post-transplantation revealed changes in bone volume and morphology of transplanted fragments as well as the presence of cardiotoxin-induced HO. Bone volume (mm^3) was quantified for experimental (LHL) and control (RHL) samples. Within each time point shown above, the left hindlimb is the left panel and the right hindlimb is the right panel. Note: images were cropped and resized to preserve consistent sizing of anatomical landmarks.

In replicate 3, LHL HO increased from day 7 to 14 (0.0434531 mm^3 to 1.55714 mm^3), decreased to 0.550547 mm^3 at day 21, and increased again to 0.77625 mm^3 by day 28 (Figure

8A, C, E, G, I; Figure 9A-C). The blue fragment steadily decreased from day 0 (0.694828 mm^3) onwards until plateauing around day 21 at 0.450562 mm^3 (Figure 9A-C). The red fragment was 0.65475 mm^3, 0.647578 mm^3, 0.65391 mm^3, 0.521016 mm^3, and 0.421031 mm^3 at day 0, 7, 14, 21, and 28, respectively—remaining steady in volume until day 14 and decreasing at subsequent time points (Figure 9A-C). RHL HO peaked at day 21 (6.09441 mm^3) and decreased to 2.14903 mm^3 by day 28 (Figure 8B, D, F, H, J; Figure 9A-C).

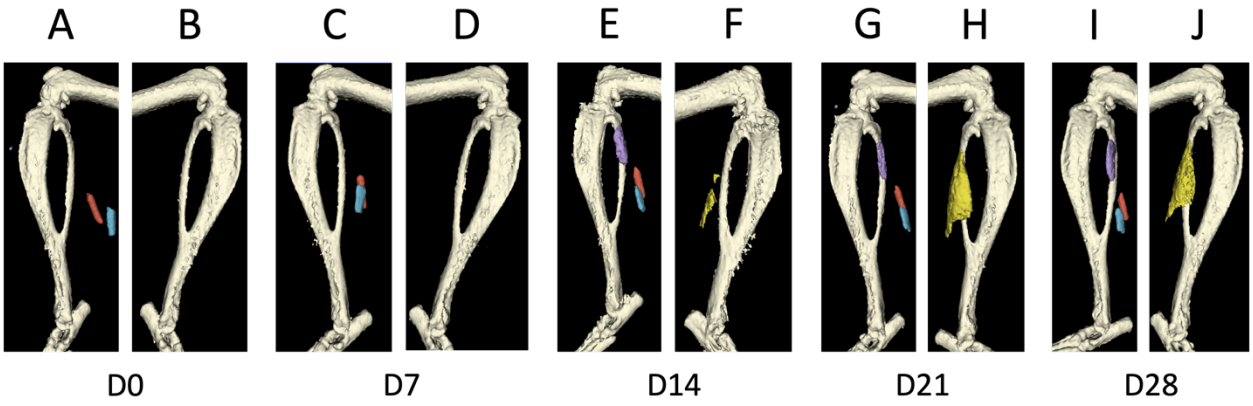

Figure 8: Replicate 3 micro-CT quantification of HO proceeding bone fragment transplantation into FOP host. Micro-CT conducted at days 0, 7, 14, 21, and 28 post-transplantation revealed changes in bone volume and morphology of transplanted fragments as well as the presence of cardiotoxin-induced HO. Bone volume (mm^3) was quantified for experimental (LHL) and control (RHL) samples. Within each time point shown above, the left hindlimb is the left panel and the right hindlimb is the right panel. Note: images were cropped and resized to preserve consistent sizing of anatomical landmarks.

A

replicate	fragment	D0 bone volume (mm^3)	D7 bone volume (mm^3)	D14 bone volume (mm^3)	D21 bone volume (mm^3)
1	blue	0.586406	0.634922	0.62859	0.424828
	red	0.381375	0.412594	0.97875	0.261141
2	blue	0.391078	0.462797	0.44086	0.251016
	red	0.385594	0.415547	0.38433	0.361547
3	blue	0.694828	0.578391	0.52650	0.450562
	red	0.654750	0.647578	0.65391	0.521016

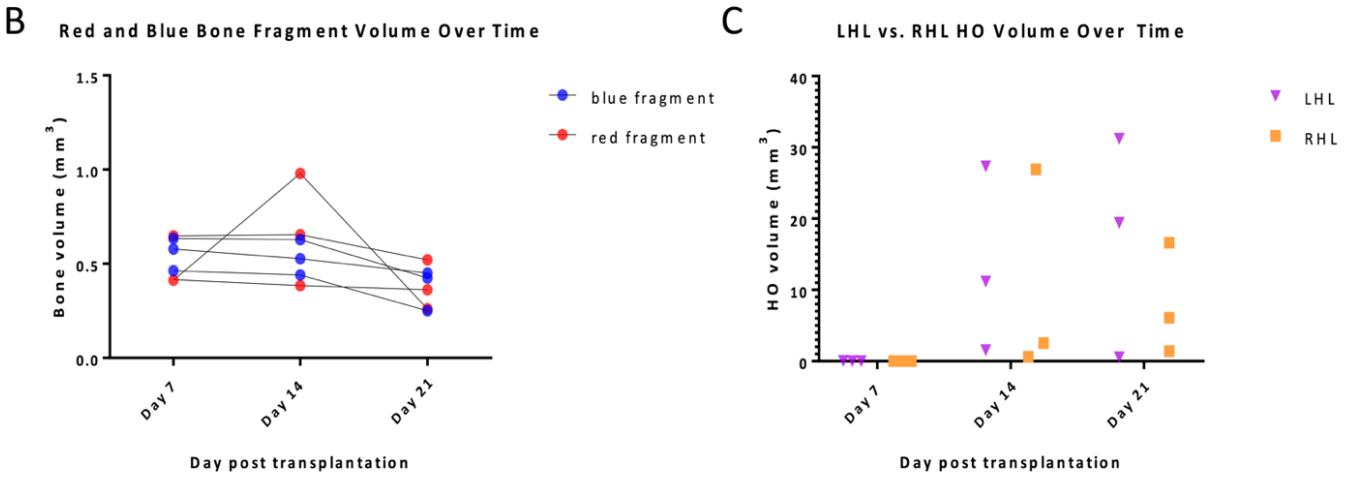

Figure 9: Tabular and graphical representations of bone volume quantification in all three replicates. Statistics and additional trials pending.

Discussion and Future Directions

The use of *Acvr1*^{tnR206H} mutant FAPs in bone fracture therapeutics has not previously been explored despite their ability to form robust HO in FOP models as well as empirical evidence suggesting their better osteogenic capacity and superior performance both in culture and *in vivo*. With nonunion fractures requiring effective and efficient bone grafts in surgical

interventions, mutant FAPs may be a viable alternative to traditional bone marrow mesenchymal stem cell therapies if properly regulated and localized to fracture sites.

While optimizing our novel bone fragment transplantation technique to model bone fractures less invasively, an early replicate (data not shown) peculiarly showed the disappearance of the bone fragment on day 7 micro-CT scans despite being present on day 0 scans. We speculated that this was due to the fragment falling out of the intramuscular pilot hole as no other replicate demonstrated this result. In subsequent experiments, careful attention was paid to ensure fragments were sufficiently embedded within the muscle and adequate skin glue was applied to close the incision site.

In our first experiment testing whether mutant FAPs colocalize with fragments in immunocompromised hosts, there was ectopic bone growth in the experimental LHL in the absence of activin A monoclonal antibody that was not highly localized to the fragment. SCID mice were empirically less resilient during surgery, some dying during the procedure which we speculate was due to prolonged isoflurane exposure. As such, mutant FAP cell injection was conducted the day after bone fragment transplantation. While this enabled the host mouse to rest and avoid prolonged anesthesia, it may have been advantageous to inject the cells into the same pilot hole containing the bone fragments as it is unclear whether HO not localizing to bone fragments was caused by insufficient BMPs or injecting mutant FAPs distant from our fracture site model. Among replicates, there was also high variability in HO formation. Cells settling in solution prior to injection was a potential source of high variability in HO in the LHL. This concern can be mitigated by using a pipette to resuspend the cells in the Eppendorf tube

directly before injection. Additionally, some solution seeped out of the hole of entry during cell injection; although the solution was extracted by the insulin syringe and reinjected, this could have caused a slightly lower concentration of mutant FAP cells being injected and potentially lower HO volumes.

To circumvent cell transplantation altogether, *Acvr1*$^{tnR206H/+}$;*R26*$^{NG/+}$;Tie2-Cre hosts were used instead so that mutant FAPs were available endogenously and only bone fragments were transplanted. Intramuscular bone fragment transplantation was not sufficient injury to induce HO as evidenced by a lack of ectopic bone in micro-CT scans weeks after transplantation (data not shown). As such, cardiotoxin was injected into both gastrocnemius muscles to stimulate mutant FAP-mediated osteogenesis proceeding sufficient muscle injury. With this method, immune rejection was a potential concern; nonetheless, micro-CT scans conducted every 7 days from day 0 to 28 post-transplantation revealed bone fragment stability. Bone volumetric data showed that replicate 1 underwent the most dramatic change in morphology with the formation of a mushroom-like cap at the end of the red fragment appearing between day 7 and 14 and disappearing between day 14 and 21. As noted, RHL HO in replicate 1 decreased from 26.9253 mm^3 to 16.6075 mm^3 while LHL HO increased from 27.3337 mm^3 to 31.201 mm^3 between day 14 and 21. We speculate that this inverse correlation may be due to an immune reaction and inflammatory response to donor fragments that contributed to the increase in HO volume between days 14 and 21. However, histological staining between these time points is pending and will provide further insights into the cell types contributing to this phenotype. While replicates 2 and 3 did not undergo as dramatic of an increase in bone fragment volume, both demonstrated fragment stability as well as changes in size and morphology. In replicate 2,

both red and blue fragments increased in volume from day 0 to day 7 but decreased steadily at all remaining time points as previously mentioned. In replicate 3, the blue fragment steadily decreased from day 0 onwards until plateauing around day 21, while the red fragment remained steady in volume until day 14 and decreased at subsequent time points. It is unclear whether this decrease in volume was due to endogenous bone resorption processes or an immune response to foreign cells without conducting histological analyses.

The lack of colocalization between transplanted bone fragments and mutant FAP-mediated HO could be due to an insufficient quantity of BMPs. While the number of fragments was altered from 1 to 2, future iterations should use a greater number of bone fragments. This was not initially conducted because of the need to introduce additional pilot holes using a thin-gauged needle at the time of transplantation. Crushing donor bone into small pieces, suspending it in solution, and injecting it intramuscularly may be another way to maximize cut bone and available BMPs. The rationale for not injecting BMPs directly despite it being the most straightforward approach was that it deviates substantially from a bone fracture model; bone fragments provide a biologically active scaffold. However, perhaps fragments can be supplemented with BMP injection, as many orthopedic surgeons have been doing since the discovery of BMPs by Urist *et al.* (Grgurevic *et al.,* 2017; Johnson *et al.,* 1988).

Furthermore, our results corroborate male-female sex differences in HO volume observed by other researchers in the lab, with females generating higher bone volumes compared to males (Apuzzo *et al*., unpublished observations). Replicates 1 and 2 were females while replicate 3 was male, and the male host generated less HO than its female counterparts.

If repeated, greater numbers of each sex should be included in our study. It is crucial to track the sex of both donor and host mice due to the sex-dependent disparity in HO seen in our mouse model of FOP.

Taken together, these data demonstrate that *Acvr1* mutant FAP-mediated, cardiotoxin-induced HO can successfully occur in our novel bone fragment transplantation assay. While HO was not localized to simulated fracture sites in both SHO-*Prkdc*^{scid}*Hr*^{hr} hosts and *Acvr1*$^{tnR206H/+}$;*R26*$^{NG/+}$;Tie2-Cre hosts, these experiments are important foundations in optimizing our intramuscular bone fragment transplantation protocol.

In addition to taking bone scans using the micro-CT, the limbs from these specimens should be collected at various time points, fixed, sectioned, and stained to observe the tissue environment at the microscopic level. Histology will reveal the spatial composition of the region between muscle and bone, where mutant FAPs (fluorescing green) localize in relation to the bone fragments, and, perhaps, miniscule bone growths undetected by micro-CT. These strategies can help determine whether mutant FAPs engrafted properly and survived as well as their exact position in the limb. Bone fragments should be collected from mice with fluorescent reporters to track lineage contribution to bone formation. In subsequent replicates, tissue should be collected for histological preparation between day 14 and 21 (when the mushroom cap morphology appeared in replicate 1) to visualize at the cellular level which cells are contributing to bone growth at the ends of fragments. Additionally, using inflammatory and immune cell-identifying markers can provide additional insights into the host's immune

response in the gastrocnemius muscle of the experimental limb proceeding bone fragment transplantation.

Before we can draw definitive conclusions about HO localization, future iterations should also incorporate the activin A monoclonal antibody (Acceleron Pharma), administered in a single, intraperitoneal injection on the day of transplantation at a dose of 10 mg/kg (Lees-Shepard *et al.,* 2018b). Additionally, while a primary aim of the present study was to design and optimize a less invasive way to model bone fractures without physically fracturing bones, an important step in between their successful adaptation to the clinic is injecting mutant FAPs directly at the site of a fracture.

Ultimately, when fractures fail to heal on their own and require surgery to repair, it is imperative that physicians provide efficient and long-term solutions to prevent further bone complications. While traditional stem cells often lose their osteogenic ability when handled in the lab, the mutant FAP cell model that my project seeks to test could solve such issues. Above all, ensuring that bone cell formation is strictly localized to the fracture site will be crucial to bringing this idea from the bench top to the operating room.

References

Biswas AA, Goldhamer DJ. FACS Fractionation and Differentiation of Skeletal-Muscle Resident Multipotent Tie2+ Progenitors. Methods Mol Biol. 2016;1460:255-67. doi: 10.1007/978-1-4939-3810-0_18. PMID: 27492178; PMCID: PMC8237095.

Cipriano J, Lakshmikanthan A, Buckley C, Mai L, Patel H, Pellegrini M, Freeman JW. Characterization of a prevascularized biomimetic tissues engineered scaffold for bone regeneration. *J Biomed Mater Res B Appl Biomater*. 2019;108(4):1655-1668. doi: 10.1002/jbm.b.34511.

Contreras O, Rossi FMV, Theret M. Origins, potency, and heterogeneity of skeletal muscle fibro-adipogenic progenitors-time for new definitions. *Skelet Muscle*. 2021;11(1):16. Published 2021 Jul 1. doi:10.1186/s13395-021-00265-6.

Culbert AL, Chakkalakal SA, Theosmy EG, Brennan TA, Kaplan FS, Shore EM. Alk2 regulates early chondrogenic fate in fibrodysplasia ossificans progressiva heterotopic endochondral ossification. Stem Cells. 2014 May;32(5):1289-300. doi: 10.1002/stem.1633. PMID: 24449086; PMCID: PMC4419363.

Giordani L, He GJ, Negroni E, Sakai H, Law JYC, Siu MM, Wan R, Corneau A, Tajbakhsh S, Cheung TH, Le Grand F. High-Dimensional Single-Cell Cartography Reveals Novel Skeletal Muscle-Resident Cell Populations. Mol Cell. 2019 May 2;74(3):609-621.e6. doi: 10.1016/j.molcel.2019.02.026. Epub 2019 Mar 25. PMID: 30922843.

Grgurevic L, Pecina M, Vukicevic S. Marshall R. Urist and the discovery of bone morphogenetic proteins. Int Orthop. 2017 May;41(5):1065-1069. doi: 10.1007/s00264-017-3402-9. Epub 2017 Feb 11. PMID: 28188395.

Hatsell SJ, Idone V, Wolken DM, et al. ACVR1R206H receptor mutation causes fibrodysplasia ossificans progressiva by imparting responsiveness to activin A. *Sci Transl Med*. 2015;7(303):303ra137. doi:10.1126/scitranslmed.aac4358.

Hino K, Ikeya M, Horigome K, et al. Neofunction of ACVR1 in fibrodysplasia ossificans progressiva. *Proc Natl Acad Sci U S A*. 2015;112(50):15438–15443. doi:10.1073/pnas.1510540112.

Joe AW, Yi L, Natarajan A, et al. Muscle injury activates resident fibro/adipogenic progenitors that facilitate myogenesis. *Nat Cell Biol*. 2010;12(2):153-163. doi:10.1038/ncb2015.

Johnson EE, Urist MR, Finerman GA. Bone morphogenetic protein augmentation grafting of resistant femoral nonunions. A preliminary report. Clinical Orthopaedics and Related Research. 1988 May(230):257-265. PMID: 3284678.

Kaplan FS, Chakkalakal SA, Shore EM. Fibrodysplasia ossificans progressiva: mechanisms and models of skeletal metamorphosis. *Dis Model Mech*. 2012;5(6):756-762. doi:10.1242/dmm.010280.

Kaplan FS, Le Merrer M, Glaser DL, et al. Fibrodysplasia ossificans progressiva. *Best Pract Res Clin Rheumatol*. 2008;22(1):191–205. doi:10.1016/j.berh.2007.11.007.

Kisanuki YY, Hammer RE, Miyazaki J, Williams SC, Richardson JA, Yanagisawa M. Tie2-Cre transgenic mice: a new model for endothelial cell-lineage analysis in vivo. Dev Biol. 2001 Feb 15;230(2):230-42. doi: 10.1006/dbio.2000.0106. PMID: 11161575.

Lees-Shepard JB, Nicholas SE, Stoessel SJ, et al. Palovarotene reduces heterotopic ossification in juvenile FOP mice but exhibits pronounced skeletal toxicity. *Elife*. 2018a;7:e40814. doi:10.7554/eLife.40814.

Lees-Shepard JB, Yamamoto M, Biswas AA *et al.* Activin-dependent signaling in fibro/adipogenic progenitors causes fibrodysplasia ossificans progressiva. *Nat Commun.* 2018b;9(1):471. doi.org/10.1038/s41467-018-02872-2.

Lounev VY, Ramachandran R, Wosczyna MN, et al. Identification of progenitor cells that contribute to heterotopic skeletogenesis. *J Bone Joint Surg Am*. 2009;91(3):652-663. doi:10.2106/JBJS.H.01177.

Mauro A. Satellite cell of skeletal muscle fibers. J Biophys Biochem Cytol. 1961 Feb;9(2):493-5. doi: 10.1083/jcb.9.2.493. PMID: 13768451; PMCID: PMC2225012.

Oprescu SN, Yue F, Qiu J, Brito LF, Kuang S. Temporal Dynamics and Heterogeneity of Cell Populations during Skeletal Muscle Regeneration. *iScience*. 2020;23(4):100993. doi:10.1016/j.isci.2020.100993.

Perez JR, Kouroupis D, Li DJ, Best TM, Kaplan L, Correa D. Tissue Engineering and Cell-Based Therapies for Fractures and Bone Defects. *Front Bioeng Biotechnol*. 2018;6:105. doi:10.3389/fbioe.2018.00105.

Puri MC, Bernstein A. Requirement for the TIE family of receptor tyrosine kinases in adult but not fetal hematopoiesis. Proc Natl Acad Sci U S A. 2003 Oct 28;100(22):12753-8. doi: 10.1073/pnas.2133552100. Epub 2003 Oct 6. PMID: 14530387; PMCID: PMC240690.

Scott RW, Arostegui M, Schweitzer R, Rossi FMV, Underhill TM. Hic1 Defines Quiescent Mesenchymal Progenitor Subpopulations with Distinct Functions and Fates in Skeletal Muscle Regeneration. *Cell Stem Cell*. 2019;25(6):797-813.e9. doi:10.1016/j.stem.2019.11.004.

Shen Q, Little SC, Xu M, Haupt J, Ast C, Katagiri T, Mundlos S, Seemann P, Kaplan FS, Mullins

MC, Shore EM. The fibrodysplasia ossificans progressiva R206H ACVR1 mutation activates BMP-independent chondrogenesis and zebrafish embryo ventralization. J Clin Invest. 2009 Nov;119(11):3462-72. doi: 10.1172/JCI37412. Epub 2009 Oct 12. PMID: 19855136; PMCID: PMC2769180.

Shore E, Xu M, Feldman G *et al.* A recurrent mutation in the BMP type I receptor ACVR1 causes inherited and sporadic fibrodysplasia ossificans progressiva. *Nat Genet*. 2006;38:525-527. https://doi.org/10.1038/ng1783.

Takakura N, Huang XL, Naruse T, Hamaguchi I, Dumont DJ, Yancopoulos GD, Suda T. Critical role of the TIE2 endothelial cell receptor in the development of definitive hematopoiesis. Immunity. 1998 Nov;9(5):677-86. doi: 10.1016/s1074-7613(00)80665-2. PMID: 9846489.

Uezumi A, Fukada S, Yamamoto N, Takeda S, Tsuchida K. Mesenchymal progenitors distinct from satellite cells contribute to ectopic fat cell formation in skeletal muscle. Nat Cell Biol. 2010 Feb;12(2):143-52. doi: 10.1038/ncb2014. Epub 2010 Jan 17. PMID: 20081842.

Uezumi A, Ito T, Morikawa D, Shimizu N, Yoneda T, Segawa M, Yamaguchi M, Ogawa R, Matev MM, Miyagoe-Suzuki Y, Takeda S, Tsujikawa K, Tsuchida K, Yamamoto H, Fukada S. Fibrosis and adipogenesis originate from a common mesenchymal progenitor in skeletal muscle. J Cell Sci. 2011 Nov 1;124(Pt 21):3654-64. doi: 10.1242/jcs.086629. Epub 2011 Nov 1. PMID: 22045730.

Wolken DM, Idone V, Hatsell SJ, Yu PB, Economides AN. The obligatory role of Activin A in the formation of heterotopic bone in Fibrodysplasia Ossificans Progressiva. Bone. 2018 Apr;109:210-217. doi: 10.1016/j.bone.2017.06.011. Epub 2017 Jun 16. PMID: 28629737; PMCID: PMC6706059.

Wosczyna MN, Biswas AA, Cogswell CA, Goldhamer DJ. Multipotent progenitors resident in the skeletal muscle interstitium exhibit robust BMP-dependent osteogenic activity and mediate heterotopic ossification. *J Bone Miner Res*. 2012;27(5):1004-1017. doi:10.1002/jbmr.1562.

Wosczyna MN, Konishi CT, Perez Carbajal EE, et al. Mesenchymal Stromal Cells Are Required for Regeneration and Homeostatic Maintenance of Skeletal Muscle. *Cell Rep*. 2019;27(7):2029-2035.e5. doi:10.1016/j.celrep.2019.04.074.